# Csf1R inhibition attenuates experimental autoimmune encephalomyelitis and promotes recovery

**Jillian C. Nissen**[1,#,%], **Kaitlyn K. Thompson**[1,%], **Brian L. West**[2], and **Stella E. Tsirka**[1,*]

[1]Program in Molecular and Cellular Pharmacology, Department of Pharmacological Sciences, Stony Brook University, NY 11794-8651

[2]Plexxikon, Inc., Berkeley, CA 94710

## Abstract

Multiple sclerosis (MS) is a chronic autoimmune disease of the central nervous system (CNS) characterized by progressive neuronal demyelination and degeneration. Much of this damage can be attributed to microglia, the resident innate immune cells of the CNS, as well as monocyte-derived macrophages, which breach the blood-brain barrier in this inflammatory state. Upon activation, both microglia and macrophages release a variety of factors that greatly contribute to disease progression, and thus therapeutic approaches in MS focus on diminishing their activity. We use the CSF1R inhibitor PLX5622, administered in mouse chow, to ablate microglia and macrophages during the course of experimental autoimmune encephalomyelitis (EAE), an animal model of MS. Here, we show that ablation of these cells significantly improves animal mobility and weight gain in EAE. Further, we show that this treatment addresses the pathological hallmarks of MS, as it reduces demyelination and immune activation. White matter lesion areas in microglia/macrophage-depleted animals show substantial preservation of mature, myelinating oligodendrocytes in comparison to control animals. Taken together, these findings suggest that ablation of microglia/macrophages during the symptomatic phase of EAE reduces CNS inflammation and may also promote a more permissive environment for remyelination and recovery. This microglia and macrophage-targeted therapy could be a promising avenue for treatment of MS.

[*]To whom correspondence should be addressed: Dr. Stella E. Tsirka, Department of Pharmacological Sciences, Stony Brook University, NY 11794-8651; Tel: 631-4443859; styliani-anna.tsirka@stonybrook.edu.
[#]*Current Address*: Department of Biological Sciences, State University of New York, College at Old Westbury, Old Westbury, NY 11568, USA; nissenj@oldwestbury.edu
[%]These two authors contributed equally to the work.

**DECLARATIONS:** All animal work complied with Stony Brook University guidelines, and was approved by the Stony Brook IACUC committee. All authors have seen drafts of this manuscript and consent for publication. The datasets used and analyzed during the current study are available from the corresponding author on reasonable request.

Competing Interests: BLW is employed by Plexxikon Inc., which provided the PLX5622 drug for this study. The authors have no additional financial interests.

Author Contributions: JCN designed and performed experiments, analyzed the data and wrote drafts of the manuscript. KKT designed and performed experiments, analyzed the data and wrote drafts of the manuscript. BLW provided the PLX5622 compound and performed the experiments. SET designed experiments, analyzed the data and wrote drafts of the manuscript.

## INTRODUCTION

Microglia comprise approximately 10% of cells in the central nervous system (CNS) and function as the resident immune cells that monitor the brain for injury, infection, and pathological changes (Nimmerjahn et al., 2005; Salter and Stevens, 2017). Alterations in CNS homeostasis lead to microglial activation, which is characterized by changes in cell morphology, proliferation, and production of cytokines (Kettenmann et al., 2011; Streit et al., 1999). Aberrant microglial activity has been associated with a variety of neurodegenerative disorders including multiple sclerosis, traumatic brain injury, epilepsy, stroke, and Parkinson's disease (Block et al., 2007; Salter and Stevens, 2017), and the inflammatory mediators produced by microglia in response to injury or infection are associated with poor clinical outcomes (Dheen et al., 2007). Thus, studies have focused on strategies to modulate microglial activity and numbers in hopes of developing effective disease therapeutics.

Colony stimulating factor 1 receptor (CSF1R) is a receptor tyrosine kinase that is present on microglia as well as some peripheral immune cells, predominantly monocytes and macrophages (Byrne, 1981). CSF1R stimulation by its ligands CSF1 and IL-34 regulates proliferation, differentiation, and survival of these cells (Elmore et al., 2014; Patel and Player, 2009), and mice lacking CSF1R or either ligand are viable but have few if any microglia or macrophages (Dai, 2002; Erblich et al., 2011; Li et al., 2006). PLX5622 (Plexxikon Inc.) is an oral CSF1R antagonist that inhibits its kinase activity at nanomolar concentrations (Ki = 5.9 nM) (Coniglio et al., 2012). Though kinase inhibitors are notorious for promiscuously binding multiple receptors, PLX5622 has displayed at least 50-fold selectivity for CSF1R over other related kinases, indicating that CSF1R is the most sensitive target (Dagher et al., 2015). When mixed into standard rodent chow PLX5622 rapidly depletes virtually all microglia within seven days. Microglia can fully repopulate the CNS within several days after drug withdrawal (Dagher et al., 2015; Huang et al., 2018). PLX5622 and a related compound that inhibits c-Kit in addition to CSF1R (PLX3397) are thought to be effective at ablating microglia, while leaving macrophages in the spleen unaffected (Hilla et al., 2017; Szalay et al., 2016). However, studies have observed a decrease in macrophages outside the CNS at the sites of peripheral nerve inflammation in partial sciatic nerve ligation (Lee et al., 2018) and mouse models of Charcot-Marie-Tooth neuropathy (Klein et al., 2015). Preclinical reports have proposed PLX5622 as a potential therapeutic for a range of diseases in which microglia and/or macrophages are implicated, including Alzheimer's disease (Dagher et al., 2015), HIV infection (Cunyat et al., 2016), and neuropathic pain (Lee et al., 2018); further, the inhibitor has been shown to prevent brain-irradiation induced memory deficits (Feng et al., 2016).

Here we focus on multiple sclerosis (MS), a chronic autoimmune disorder of the CNS that affects over 2.5 million people worldwide. MS and experimental autoimmune

encephalomyelitis (EAE), an MS animal model, are characterized by progressive demyelination and degeneration of neurons (Swanborg, 1995). Microglial activation is an early event in MS/EAE that persists throughout, and strongly influences, the disease course (Zhang et al., 2011). Monocyte-derived macrophages, which constitute a significant portion of the massive peripheral immune cell infiltrate found in the CNS in MS/EAE, also modulate disease progression and have been shown to be largely responsible for the effector phase of EAE (Ajami et al., 2011; King et al., 2009; Mildner et al., 2009). Upon activation, both microglia and macrophages release pro-inflammatory cytokines that are associated with active demyelination and more severe mobility impairment and larger white matter lesions (Mikita et al., 2011; Zrzavy et al., 2017). Further, proinflammatory microglia and macrophages have been associated with transected axons (Bogie et al., 2014; Trapp, 1998). Thus, both microglia and monocyte-derived macrophages strongly influence the MS disease course (O'Loughlin et al., 2018) and modification of these cells is a promising strategy for ameliorating MS symptoms.

Previously, microglial inactivation using the CD11b-HSVTK transgenic mouse was observed to produce a significant reduction in EAE severity (Heppner et al., 2005). Similarly, selective depletion of inflammatory CCR2+Ly6C$^{hi}$ monocytes resulted in attenuated EAE (Mildner et al., 2009). While these data are encouraging conceptually, transgenic models of depletion are not translatable to human patients.

In this study, we sought to determine the potential of pharmacological ablation of microglia and monocytes/macrophages as a therapy for MS. We show that CSF1R inhibition via PLX5622 rapidly depletes these cells in the spinal cord and significantly ameliorates EAE symptoms. Further, the small number of microglia/macrophages that remain following ablation shift towards a more anti-inflammatory, neuroprotective phenotype. Treatment with PLX5622 also results in the retention of mature, myelinating oligodendrocytes in white matter lesions, as opposed to control animals, where primarily oligodendrocyte progenitor cells are observed. Finally, we show that continuous CSF1R inhibition during symptomatic phases is important to ascertain that EAE symptoms remain attenuated.

## MATERIALS AND METHODS

### Animals and Food

Female C57BL6 mice (8–10 weeks old) utilized in this study were bred in-house under pathogen-free conditions. Food and water were accessible *ad libitum*, and all animals were on a 12-hour light/dark cycle. PLX5622 was obtained from Plexxikon, Inc. and was mixed into AIN-76A control chow by Research Diets, Inc. Mice were fed normal control chow for 7 days after induction of EAE, at which point they were switched to food containing the PLX5622 drug or comparable drug-free control food for the remainder of the experiment. PLX5622 was administered in two doses – high dose food contained 1,200 mg PLX5622 per kilogram of food, and low dose contained 300 mg/kg PLX5622. After two weeks of drug administration, PLX5622 was detectable in both plasma and in brain tissue, with the high dose treated animals reaching a concentration approximately double of those treated with low dose PLX5622 (Table S1).

### Induction of EAE with MOG$_{35-55}$ Peptide

MOG$_{35-55}$ peptide (MEVGWYRSPFSRVVHLYRNGK) was purchased from Biomatik USA, LLC (Wilmington, DE). EAE was induced in female mice (8–10 weeks old) by subcutaneous injection in the hind flank on day 0 and day 7 with 300 μg of MOG$_{35-55}$ emulsified in complete Freund's adjuvant (CFA) containing 500 μg of heat-inactivated *Mycobacterium tuberculosis* (Difco, Detroit, MI) (Bhasin et al., 2007; Nissen and Tsirka, 2016; Wu et al., 2012). Five hundred nanograms of Pertussis toxin (List Biologicals, Campbell, CA) in 200 μL of PBS was injected intraperitoneally on days 0 and 2. After immunization, mice were observed daily and weighed weekly. The severity of disease symptoms was scored on a scale ranging from 0 to 5 with 0.25 gradations for intermediate symptoms. The scores are defined as follows (Hjelmstrom, 1998): 0, no detectable symptoms; 1, loss of tail tone; 2, hindlimb weakness or abnormal gait; 3, complete hindlimb paralysis; 4, complete hindlimb paralysis with forelimb weakness or paralysis; 5, moribund or dead. Investigators were blinded to the treatments during the experiment.

### Tissue Collection and Processing for Histopathology

Mice were anesthetized with an intraperitoneal injection of 2.5% avertin (0.02 mL/g body weight) and transcardially perfused using PBS (pH 7.4) followed by 4% paraformaldehyde (PFA) in PBS (pH 7.4). Spinal cords were isolated, post-fixed in 4% PFA, and dehydrated in 30% sucrose. After removing the meninges, the spinal cord was cut into 6 equal sections, embedded in optimal cutting temperature (OCT) compound (Tissue Tek), frozen, and stored at −80°C. Tissue was sectioned at 20μm on a cryostat prior to staining.

### Immunofluorescence

Spinal cord sections mounted on slides for immunofluorescence were rinsed in PBS for 5 min to remove residual OCT. After washing, samples were blocked in serum of the host of the secondary antibody (5% serum and 0.3% BSA in PBS with 0.2% Triton-X 100) and then incubated overnight with rabbit anti-mouse Iba1 (1:500, Wako), mouse anti-mouse iNOS (1:500, BD Biosciences), mouse anti-mouse Arg-1 (1:500, BD Biosciences), rat anti-mouse CD86 (1:500, BD Biosciences), goat anti-mouse CD206 (1:100, R&D Systems), rabbit anti-mouse GFAP (1:1000, Dako) rabbit anti-mouse NG2 (1:500, a generous gift from the Levine lab), mouse anti-mouse CC1 (1:100, EMD Millipore), rat anti-mouse MBP (1:50, Bio-Rad), or rabbit anti-mouse neurofilament-L (1:100, EMD Millipore) in 0.3% BSA in PBS with 0.2% Triton-X 100. After washing with PBS, sections were incubated with fluorescence-conjugated FITC or Cy3 goat anti-rabbit, goat anti-mouse, goat anti-rat, or donkey anti-goat antibody for 1 h at room temperature, washed three times with PBS, and mounted using Fluoromount-G with DAPI (Southern Biotech, USA). The sections were imaged using a Nikon Eclipse E600 microscope and Zeiss LSM 510 confocal microscope.

### Eriochrome cyanine staining

Eriochrome cyanine (EC) staining was used to visualize myelin in the lumbar region of the spinal cord as we have previously described (Wu et al., 2012). In brief, spinal cord sections previously stored at −80°C were air-dried overnight at room temperature. The sections were then incubated at 37°C for 2 hours in a dry incubator. After incubation with acetone for 5

minutes, the slides were air-dried for 30 minutes and then stained in EC solution (0.2% eriochrome cyanine RS (Sigma), 0.5% $H_2SO_4$ (Sigma), 10% iron alum (Sigma) in distilled water) for 30 minutes, differentiated in 5% iron alum (Sigma) for 10 minutes, and placed in borax-ferricyanide solution (1% borax (Sigma), 1.25% potassium ferricyanide (Sigma), in distilled water) for 5 minutes. The slides were then dehydrated through graded ethanol solutions and coverslipped using Permount (Fisher Scientific, NJ, USA). The stained sections were then imaged on a Nikon Eclipse E600 microscope at 40x magnification. ImageJ freeware (NIH) was used to measure the demyelinated and total areas of the white matter. In brief, images were cropped to remove the gray matter regions prior to quantification. To distinguish between positive-staining white matter areas and demyelinated regions, thresholding was used to obtain a binary signal. The demyelinated area was determined by subtracting the myelinated region from the total area, and percentage was calculated as shown below. Six full coronal sections were analyzed for each biological replicate.

$$\text{Demyelinated area}\ (\%) = (\text{Demyelinated area in white matter} / \text{Total white matter area}) * 100\%$$

### Flow Cytometry

To analyze immune cell populations in the spinal cord, spleen, and blood, MOG-EAE was induced as explained above. The mice then received either control chow or chow containing 1,200 mg/kg PLX5622 on Day 14, to model a therapeutic treatment timeline more relevant to clinical applications. On Day 18, mice were euthanized by avertin injection and cardiac puncture was performed to collect blood. The spleen and the spinal cord were then isolated.

The blood was collected in a heparinized syringe and 100 uL of whole blood was blocked with CD16/32 Fc block (Biolegend, 1:50 in FACS buffer) for 30 minutes and stained with CD11b-APC (Biolegend, 1:100), CD45-PerCP-Cy5.5 (Biolegend, 1:100) and Ly6C-FITC (Biolegend, 1:100) in FACS buffer for 30 minutes. This was followed by incubation with 1-step Fix/Lyse (eBioscience) for 30 minutes and 1 wash in FACS buffer.

The spleen was isolated and pressed through a 70um cell strainer to create a single cell suspension. Splenocytes were treated with ACK lysing buffer (0.15 M $NH_4Cl$, 10 mM $KHCO_3$, 0.1 mM $Na_2$-EDTA) for 5 minutes on ice to lyse red blood cells. Cells were then rinse and counted using trypan blue exclusion on a hemocytometer. Suspended cells were blocked using anti-mouse CD16/32 Fc block (Biolegend, 1:50 in FACS buffer) and stained with CD11b-APC (Biolegend, 1:100), CD86-Pacific Blue (Biolegend, 1:100), CD206-PE (Biolegend, 1:100), and MHCII-FITC (Biolegend, 1:100). After two rinses with FACS buffer, cells were fixed in 4% PFA (Biolegend), washed twice with FACS buffer, and re-suspended for analysis.

The spinal cord was digested in 1 mg/mL papain (Sigma) and triturated for mechanical dissociation. Following removal of the papain solution, 30% Percoll (Sigma) was added to remove myelin debris by density centrifugation. Cells were rinsed twice in HBSS and blocked with CD16/32 Fc block (Biolegend, 1:50 in FACS buffer) for 30 minutes. Cells were then stained with CD11b-APC (1:100), CD86-Pacific Blue (1:100) and CD206-PE

(1:100) (Biolegend) or with CD3-Pacific Blue (1:100) and CD4-PerCP (1:100) for 30 minutes. After two rinses with FACS buffer, cells were fixed in 4% PFA (Biolegend). For analysis of Th subsets, following fixation, cells were permeabilized with 1x Permeabilization Wash Buffer (Biolegend) by rinsing 3 times, blocking for 30 minutes on ice (1:50 Fc block in 1x Permeabilization Wash Buffer) and staining with IFN$\gamma$-FITC (Biolegend, 1:100 in 1x Permeabilization Wash Buffer) and IL-17a-PE (Biolegend, 1:100 in 1x Permeabilization Wash Buffer) for 1 hour on ice. Cells were rinsed twice more in Permeabilization Wash Buffer and re-suspended in FACS buffer for analysis.

Analysis was performed on a BD LSR Fortessa and post-processed on FlowJo.

### Experimental Design and Statistical Analysis

To analyze the effect of CSF1R inhibition on the physical hallmarks of EAE, female C57BL/6 animals were utilized (control: 12 animals, PLX5622 high: 16 animals, PLX5622 low: 14 animals) and pooled from 6 different experiments. These were scored for 28 days, and changes in disease score and weight were analyzed by a two-way ANOVA followed by a Bonferroni post-test. Peak score was recorded as the highest score reached over 28 days, cumulative score was the sum of the scores of 28 days, and statistics were determined by a two-tailed t test using GraphPad Prism. For withdrawal experiments, three animals were used per treatment group.

For quantification of myelination and global microglia and macrophage activation, tissue was collected from 3 or 4 animals per treatment group (control, PLX 5622 high/low) on days 9, 14, 21, and 28. Three uninjured wild-type animals were collected at day 0 as a baseline control. 6 full coronal sections from the lumbar spinal cord were stained and imaged as described above. Results were analyzed by a two-tailed t test using GraphPad Prism.

To investigate microglial polarization and oligodendrocyte dynamics, tissue was collected from 3 animals per treatment group (control, PLX 5622 high/low) on days 14, 21, and 28. Three uninjured wild-type animals were collected at day 0 as a baseline control. Six images from within the white matter of the lumbar spinal cord were collected following staining, and analyzed by a two-tailed t test using GraphPad Prism.

All results are represented as the mean with error bars indicating the standard error of the mean.

## RESULTS

### CSF1R inhibition improves mobility and reduces weight loss in EAE

At day 7 post EAE induction, the animals exhibited mild physical impairments (Fig. 1A). Whereas the clinical symptoms progressively worsened over the following three weeks for the control animals, the animals treated with either low or high dose of PLX5622 had significantly lower disease scores. The attenuation in impairment was evident as early as two days after the administration of drug in the chow and remained through to day 28 (Fig. 1A). To quantify the effect of PLX5622 on overall well-being throughout the month of scoring, and to assess the most severe symptoms that the animals experienced, the cumulative and

peak scores were analyzed, respectively. Control animals had a cumulative score of 36.56 ± 1.71, which was significantly higher than that of animals treated with the low dose (8.79 ± 3.51) or high dose (7.20 ± 3.83) food, indicating improved overall well-being (Fig. 1B). Peak scores followed a similar trend, where control animals peaked at 3.03 ± 0.18, indicative of full hindlimb paralysis, while low dose-treated animals had only a limp tail (1.52 ± 0.24). This was even more dramatically displayed for the high dose-treated group, where the only impairment observed was in curling the tip of their tail (0.78 ± 0.01) (Fig. 1C). Taken together these behavioral outcomes demonstrate that ablation of CSF1R+ cells using PLX5622 significantly reduced EAE severity.

For MS patients weight loss parallels the severity of motor symptoms (Emerson et al., 2009). In EAE we recorded animal weights weekly as an indicator of disease severity. It has been previously shown that PLX5622 does not impact mouse daily food intake (Valdearcos et al., 2014), and therefore changes in weight can be attributed to improved EAE outcomes rather than reduced consumption of the drug-containing food. While control animals steadily lost weight over the 28 days of scoring, animals treated with either dose of PLX5622 showed significant improvement in weight loss compared to controls, nearly returning to their pre-EAE weights (Fig. 1D). These results indicate that CSF1R inhibition by PLX5622 can effectively improve physical impairments in EAE that parallel the hallmarks of MS.

To understand the rapid decrease in the severity of motor symptoms of PLX5622-treated mice after only 2 days of treatment, we performed a histological evaluation of the tissue at that time point. Demyelination and inflammation in the spinal cord of mice were assessed nine days post-induction of EAE (animals were administered control chow or chow containing 1,200 mg/kg PLX5622 on day 7). No differences were evident in demyelination (control: 5.81% ± 0.55, PLX5622 high dose: 5.28% ± 0.26), visualized by eriochrome cyanine (EC) staining (Fig. 2A, B), in the white matter of the lumbar spinal cord region 2-days post treatment.

Inflammation and the extent of microglia/macrophage depletion in the CNS were examined by assessing the number of Iba1+ microglia and macrophages in the lumbar spinal cord region (Fig 2C). It has been previously reported that the 1,200 mg/kg dose of PLX5622 eliminates ~80% of microglia within 7 days (Dagher et al., 2015). Here, after only two days of PLX5622 treatment at the 1,200 mg/kg dose, we observed a ~40% decrease in the number of microglia/macrophages in the spinal cord (Fig. 2D) (control: 7.79 ± 0.91, PLX5622 high dose: 3.06 ± 0.48). This result suggests that the rapid and significant improvement in motor deficits can be attributed to partial depletion of microglia and macrophages in the spinal cord and thus, decreased CNS inflammation in PLX5622-treated animals.

To evaluate whether peripheral macrophages were affected by PLX5622 treatment at this early time point we examined Iba1 staining in the spleen (Fig. 2E). There were no differences in the intensity of the Iba1 signal (Fig 2F) (control: 5.67 ± 1.06, PLX5622 high dose: 5.53 ± 0.32) or the percent area positive for Iba1 staining (Fig. 2G) (control: 13.26% ± 0.97, PLX5622 high dose: 12.06% ± 0.10), indicating that effects of PLX5622 in the periphery are not as rapid as in the inflamed CNS.

## The microglia and macrophages that remain in the spinal cord after depletion are shifted away from inflammatory phenotypes

We next sought to determine the efficiency with which PLX5622 treatment depleted CSF1R + cells during EAE. Coronal sections of the lumbar region of the spinal cord were immunostained for Iba1, a marker for both microglia and macrophages. We quantified the Iba1 signal within the entire section including gray and white matter to show that this depletion was global rather than localized to regions of microglial activation. High-dose PLX5622 significantly depleted microglia/macrophages at all time-points, whereas low-dose PLX5622 decreased microglial/macrophage numbers throughout the spinal cord but did not reach significance until day 21 (Fig. S1). The ablation was even more dramatic when analysis was restricted to white matter regions, as both doses of the drug at all time-points very significantly reduced microglial numbers (Fig. 3A, B). PLX5622 treatment did not result in astrogliosis, since no increase in GFAP expression following CSF1R inhibition was visible (Fig. S2), which is consistent with previous reports regarding astrocyte numbers after administering the CSF1R/c-Kit inhibitor PLX3397 (Elmore et al., 2014).

Although microglia/macrophages are primarily attributed detrimental roles in MS/EAE, they also promote repair once damage has occurred. This multitude of behaviors is due to their ability to polarize along a spectrum of activation states between an inflammatory, neurodegenerative phenotype which accompanies worsened MS/EAE symptoms, and a neuroprotective, anti-inflammatory phenotype. Inflammatory microglia and macrophages dominate in the CNS in the early stages of EAE, but then anti-inflammatory populations are predominant during recovery (Kigerl et al., 2009). Although administration of PLX5622 results in widespread elimination of microglia and macrophages in the spinal cord, some cells do remain, especially in the animals fed low-dose PLX5622. As animals treated with high-dose PLX5622 had almost no Iba1+ cells remaining, all analysis for polarization was potentially skewed by small sample size, and is thus included as Fig. S3. As the balance between pro- and anti-inflammatory phenotypes strongly affects the MS/EAE disease course (Mikita et al., 2011), we sought to determine both the microglia and monocyte-derived macrophage state following PLX5622 treatment. Tissues were stained with Iba1 to visualize microglia and macrophages, iNOS to mark inflammatory cells, and arginase-1 (Arg1) to detect anti-inflammatory cells. Administration of PLX5622 at low and high doses significantly reduced the percentage of predominantly inflammatory Iba1+ cells at all time-points (Fig. 3A, C). In contrast, there were almost no significant changes in the percentage of cells that were Arg1-positive and hence anti-inflammatory (Fig. 3A, D). These phenotypes were recapitulated with the additional pro-inflammatory marker CD86 and anti-inflammatory marker CD206 (Fig. S3). Nonetheless, the decrease in inflammatory microglia and macrophages would result in a less damaging, disease-promoting milieu following PLX5622 treatment (Fig. 3E, F).

## Spinal cord demyelination is reduced following CSF1R inhibition

Demyelinated lesions in the brain and spinal cord are characteristic pathologies of MS and EAE. To visualize myelin in the white matter of the spinal cord, sections were stained with EC. Demyelination was evident at day 14 in control animals ($8.96 \pm 1.16\%$), peaked by day 21 ($30.29 \pm 4.23\%$), and persisted through day 28 ($27.71 \pm 2.60\%$). Treatment with PLX5622

at high doses resulted in significantly less demyelinated white matter area at all time points (day 14, 2.21±0.098%; day 21, 7.95±0.80%; day 28 8.23±0.77). Low-dose treatment produced significant changes in lesion size at day 14 (4.65±1.00%) and 28 (9.54±0.63%) (Fig. 4). Demyelination in both low- and high-dose treatments parallels their disease course, as animals treated with high-dose PLX5622 maintained a low behavioral score between day 21 and 28 (Fig. 1), while low-dose treated animals show reduced scores at day 28, compared to day 21, indicative of disease recovery. In contrast, there was no evidence of remyelination and recovery in control animals by day 28. Thus acute, pharmacological microglial depletion ameliorates the pathological hallmarks of EAE.

We also examined more closely the association of demyelination with axonal integrity, by visualizing the presence of myelin basic protein (MBP) and neurofilament-L (NF-L) immunofluorescence in the ventral white matter of the spinal cord (Fig. S4). At day 21, spinal cord sections of control mice exhibited low MBP staining, paralleling the diminished EC staining in these animals. We also observed diffuse NF-L staining indicating some degree of axonal disruption. Mice treated with high dose PLX5622 displayed organized and intact axonal structures neatly wrapped by myelin. The PLX5622 low dose-treated mice also exhibited some MBP and NF-L disorganization, though not as notable as the control mice.

## CSF1R inhibition increases mature oligodendrocyte numbers in EAE

While reduction of inflammation is essential to prevent any further demyelination and neurodegeneration and constitutes the target of disease-modifying MS drugs, it is also important for therapies to promote remyelination and repair of white matter lesions. Mature oligodendrocytes are responsible for myelinating neurons throughout the CNS. A major source of these cells is oligodendrocyte precursor cells (OPCs), which migrate to lesion sites during MS and EAE (Gensert and Goldman, 1997; Huang et al., 2011). To visualize oligodendrocyte lineage dynamics during the EAE disease course and assess the differentiation state and numbers of oligodendrocyte lineage cells following EAE induction, we stained tissue sections for either NG2, a marker of OPCs, or CC1, a marker for mature oligodendrocytes. Control mice responded to EAE progression by increasing the numbers of NG2+ OPCs by day 14, and dramatically more so at day 21; in contrast, OPC numbers were not significantly increased at any time point following CSF1R inhibition (Fig. 5B, C). Conversely, the numbers of CC1+ mature oligodendrocytes were higher in the PLX5622-treated animals at days 14 and 28, with a stronger response observed for the high dose-treated mice (Fig. 5B, D). Since the raw numbers of oligodendrocyte lineage cells may be skewed by the fact that OPCs are recruited to MS lesion sites (Chang et al., 2000; Chang et al., 2002; Di Bello et al., 1999), we assessed the ratio of mature (CC1+) to immature (NG2+) oligodendrocytes, as the presence of more mature cells signifies increased capacity for myelination. At all three time-points examined post-EAE induction, the ratio of mature to immature cells was decreased in control animals, demonstrating their reduced capacity for recovery and repair (Fig. 5E), while the CSF1R-inhibited animals presented with more mature oligos. These results are consistent with the minimal demyelination present in the white matter of the animals treated with PLX5622 (Fig. 4).

To confirm that the NG2-positive cells were progenitors and not other NG2-glia (Nishiyama et al., 2009), co-staining tissue from day 28 with the pan-oligo marker Olig2 along with CC1 was performed. In these conditions Olig2+CC1− cells would be considered progenitors. The results of this co-staining supported the analysis above (Fig. 5F). The shift in oligodendrocyte populations from a predominance of more immature cells to more mature cells following pharmacological CSF1R inhibition treatment could explain why control animals show minimal recovery despite having higher raw numbers of oligodendrocyte lineage cells in their white matter lesions.

## Continuous CSF1R inhibition during symptomatic phases is necessary for attenuated symptoms

To determine if acute depletion of microglia/macrophages with PLX5622 suffices to achieve long-term amelioration of EAE, we induced EAE as in Fig. 1, but included a group of animals that were fed the high-dose CSF1R inhibitor for days 7–14, and then reverted to control food for the remainder of the experiment. We found that EAE symptoms began to appear within 5–6 days following drug withdrawal, and the animals reached scores indistinguishable from untreated controls 10 days following drug withdrawal (Fig. 6A). Control animals take approximately two weeks to reach their peak scores, as onset of symptoms generally occurs at day 7 post induction and the most severe symptoms emerge around day 21 (day 19, in Fig. 6A). This was also the case when PLX5622 was withdrawn, as the drug was removed on day 14 and animals reached a peak comparable to controls between days 19 and 23, and decreased to baseline at the same rate (Fig. 6A). At Day 50, Iba1+ cells in the spinal cord were comparable to those present in control, whereas there were no Iba1+ microglia/macrophages in the mice maintained on PLX5622 high dose for the duration of the experiment (Fig. 6B). These data indicate that a short treatment with PLX5622 does not suffice to prevent the development of EAE, but rather administration of PLX is important during the symptomatic phase of EAE; how long a PLX treatment would be needed has not been determined.

## Therapeutic treatment with PLX5622 rapidly attenuates EAE symptoms and depletes microglia but not macrophages

We show that administration of 1,200 mg/kg PLX5622 starting on Day 7 almost completely abolished EAE symptoms (Fig. 1A). To investigate the effects of CSF1R inhibition after the emergence of physical deficits, we initiated a therapeutic treatment with the high dose of PLX5622 starting on Day 14. At this time point, before starting control chow or chow containing PLX5622, all mice exhibited obvious signs of ascending paralysis, including a limp tail and hind limb weakness. Within three days of treatment, mice receiving PLX5622 displayed significantly less severe symptoms compared to mice receiving control chow (Fig. 7A). These results are similar to what we observed on Day 7, where significant differences in EAE symptoms emerged only two days after the start of CSF1R inhibition (Fig. 1A).

At Day 18, as PLX5622-treated mice displayed sustained attenuation of symptoms and control mice exhibited increasingly severe disease scores, we performed flow cytometric analysis to determine the effects of the CSF1R inhibitor on immune cell populations in the CNS and in the periphery.

We first validated the immunofluorescence findings of reduced microglia/macrophages in the spinal cord using the markers CD11b and CD45. Microglia were assessed as CD11b +CD45$^{int}$ cells, and macrophages were CD11b+CD45$^{hi}$. While there was no decrease in the number of macrophages at this time point (Fig. 7E), there was a significant reduction in total microglia present in the spinal cord 4 days into the therapeutic treatment regimen (Fig. 7B). We also evaluated MHCII expression on microglia and macrophages in the spinal cord. A reduction in total number of MHCII+ microglia was evident (Fig. 7C), however, the percentage of CD11b+CD45$^{int}$ cells expressing MHCII did not change (Fig. 7D), indicating that PLX5622 ablates MHCII+ microglia, but has no direct or rapid effects on MHCII expression during EAE. Macrophage MHCII expression was unchanged (Fig. 7F & G).

Since EAE is primarily mediated by T helper (Th) cells (Robinson et al., 2014), we also examined if CSF1R inhibition has effects on the presence of CD4+ T cells in the spinal cord and Th phenotype, particularly the pathogenic Th1 and Th17 subsets. We used IFNγ and IL-17a to distinguish them, respectively. We observed no differences in total CD3+CD4+ cells in the spinal cord of PLX5622-treated animals (Fig. 7H). Moreover, there were no alterations in pathogenic T-cell subsets during CSF1R inhibition (Fig. 7I).

Lastly, we examined monocyte/macrophage populations in the spleen and blood. There were no differences in splenic CD11b+ cells in PLX5622-treated mice compared to control mice (Fig. 7J). The phenotypes of these macrophages were unaffected by CSF1R inhibition (Fig. S5). Finally, CD11b+Ly6C$^{hi}$ and CD11b+Ly6C$^{lo}$ populations in peripheral blood remained unaltered by PLX5622 as well (Fig. 7K).

## DISCUSSION

Here, we present data using both low and high doses of the CSF1R inhibitor, PLX5622, as a therapeutic treatment for EAE. Although both doses attenuate disease symptoms and pathology across a variety of parameters, use of the higher dose therapy showed more significant benefits in disease scores, peak scores (Fig. 1), and white matter microglia/ macrophage depletion (Fig. 3) when administered 7-days post-MOG immunization. Importantly, we also show that high dose of PLX5622 works rapidly and effectively when administered at a later point in the disease course (Day 14), which is more relevant to patient treatment timelines as there is more obvious emergence of symptoms (Fig. 7A). Despite this, the low-dose drug may be preferred as a long-term therapy, as it does not fully ablate all microglia and macrophages in the inflammatory CNS setting (Fig. S1, S2). Microglia play an essential role in maintaining brain homeostasis and responding to injury (Nimmerjahn et al., 2005), and thus complete ablation could present unwanted consequences if individuals experienced CNS damage or infection following the onset of therapy. On the other hand, chronic treatment with PLX3397, an inhibitor of CSF1R and c-Kit, has been shown to only have modest effects on macrophage numbers in other tissues (Mok et al., 2014; Szalay et al., 2016). In fact, deletion of CSF1R does reduce macrophage numbers (Li et al., 2006), but has not been seen to abolish them completely, in contrast to the dramatic effects it has on microglia (Erblich et al., 2011). In agreement with these reports, we observed no changes in splenic macrophages two days post-initiation of high dose PLX5622, when there were already significant decreases in microglial numbers in the CNS. Further, we did not see any

changes in macrophage number or phenotype in the spleen and Ly6C$^{hi}$ or Ly6C$^{lo}$ monocytes in blood 4 days into continuous CSF1R inhibition. Therefore, patients undergoing continuous PLX5622 therapy would potentially still have peripheral monocytes/ macrophages to respond to CNS insults. Indeed, other therapies that focus on inhibition of CSF1R signaling without microglial depletion have been shown to have disease-modifying effects in EAE when given prophylactically (Borjini et al., 2016). These data also raise the question of whether Iba1+ cells observed in the spinal cord of low-dose depleted animals are in fact microglia, or whether, instead, are infiltrating peripheral cells. On this point, when we administered the high dose of PLX5622 therapeutically, we observed that microglia were rapidly depleted in the CNS within four days of treatment, however, infiltrating monocyte-derived macrophages remained unchanged (Fig. 7B & 7E). Thus, PLX5622 may preferentially deplete microglia over macrophages in the inflammatory CNS setting at lower doses or with less than one week of treatment.

Our data indicate that M1-like microglia were more sensitive to PLX treatment than were anti-inflammatory M2-like cells. Although this finding does not agree with some of the data presented in other reports when PLX3397 had been used (Mok et al., 2014), it is consistent with the data presented by Dagher et al. (Dagher et al., 2015) and Lee at al. (Lee et al., 2018) who also used PLX5622 in the disease model.

Withdrawal of PLX5622 resulted in a rapid re-emergence of EAE symptoms, leading eventually to peak scores comparable to those observed in control animals (Fig. 6). The scores began to increase 5–6 days after removing the drug, which correlates with previous studies that show return of microglia to endogenous levels within several days after genetic ablation (Bruttger et al., 2015) or after PLX5622 removal (Dagher et al., 2015; Huang et al., 2018). This rapid recovery may be due to repopulation of microglial cells. Initially, the repopulated cells were thought to emerge from a nestin-positive progenitor (Elmore et al., 2014), but more recently it was shown that they arise from residual microglia and that the newly repopulated cells only transiently-express nestin (Huang et al., 2018). The local origin of these cells would allow for faster recovery, than would be the case with peripheral monocyte infiltration. Although peripheral monocytes contribute to inflammation and damage during EAE, they are not detectable in the CNS during disease remission and do not contribute to the resident microglial pool (Ajami et al., 2011; King et al., 2009; Mildner et al., 2009). Previous studies in our lab have shown that repopulating microglia, following PLX drug withdrawal, function similarly to endogenous microglia, as they revert behavioral deficits resulting from depletion (Torres et al., 2016). Microglia are highly sensitive to injury, they respond to blood-brain barrier damage within 2 minutes (Nimmerjahn et al., 2005) and can be found clustered in normal-appearing white matter prior to any demyelination occurring in EAE and MS (Melief et al., 2013). These data could explain how microglia can revert to their inflammatory state so rapidly following repopulation, as even high-dose depleted animals have some degree of white matter demyelination. These results are intriguing, since they support the idea of microglia as a highly plastic, rapidly responsive cell population. EAE scores begin to increase only three days following drug withdrawal, which coincides with the time when microglial cells have begun to repopulate the CNS (Fig. 6) (Dagher et al., 2015). Animals treated with high-dose PLX5622 have minimal demyelination at all time points following EAE induction (Fig. 4), which implies that these

newly generated microglia can activate and induce a degenerative inflammatory response almost immediately upon their reappearance.

Surprisingly, the animals with the worst EAE symptoms also had the highest number of oligodendrocyte lineage cells in their white matter (Fig. 5). Since oligodendrocyte lineage cells do not express CSF1R, it is unlikely that the PLX5622 drug, an inhibitor of CSF1R kinase activity, had a direct impact on the cells (Luo et al., 2013; Murase and Hayashi, 1998). OPCs become recruited in MS/EAE lesions (Chang et al., 2000; Chang et al., 2002; Di Bello et al., 1999) and do not gather in normal-appearing white matter (Reynolds et al., 2002). Following the EAE disease course, OPC levels go back to control after remyelination has taken place (Di Bello et al., 1999). OPCs can differentiate into mature, myelinating oligodendrocytes in lesion sites (Chang et al., 2002; Reynolds et al., 2002; Zawadzka et al., 2010), which is consistent with what we observed at day 21 in the control animals. The numbers of CC1+ cells were not different at day 21, potentially because the OPCs that migrated into the lesion sites and differentiated into mature oligodendrocytes in the control animals were temporarily able to staunch the mature oligodendrocyte loss. OPCs also proliferate in response to demyelination (Levine, 1994). This could explain why OPCs are present in higher numbers in control animals than in the animals treated with CSF1R inhibitor, as the demyelination is much more extensive in controls. The reduction in OPCs and mature oligodendrocytes in control animals at day 28 after the induction of EAE could be due to the fact that because cells of this lineage are depleted in chronic EAE lesions (Reynolds et al., 2002), this repair mechanism was not adequately functional by day 28, when there were insufficient numbers of OPCs to address the loss of mature oligodendrocytes. Further, anti-inflammatory microglia drive oligodendrocyte differentiation during CNS remyelination (Miron et al., 2013), which could explain the abundance of mature oligodendrocytes in PLX5622-treated animals.

Taken together, our work provides support for the development of PLX5622 as a therapeutic for MS. The ability of this drug to rapidly and efficiently deplete microglia, yet still allow for reversion to the pre-therapy state within several days following withdrawal, provides a level of precise control over CNS inflammation that could support its use in a temporal manner, potentially administering it at the onset of a relapse and discontinuing use after the symptoms subside.

In this study, we demonstrate that systemic depletion of microglia using the orally-available CSF1R inhibitor PLX5622 significantly improves both the physical and pathological hallmarks of MS/EAE. The drug elicits a more regenerative environment through a selective enrichment of anti-inflammatory microglia and mature oligodendrocytes in lesion areas. However, our data suggest that PLX5622 needs to be administered during the symptomatic phases of EAE, and is not effective as a short-term, limited-in-time therapy, as symptoms held at bay in the presence of the drug rapidly emerge once it is discontinued.

## Supplementary Material

Refer to Web version on PubMed Central for supplementary material.

Author Manuscript

Author Manuscript

Author Manuscript

Author Manuscript

## Acknowledgments

## Abbreviations

| | |
|---|---|
| **MS** | Multiple sclerosis |
| **CNS** | Central nervous system |
| **CSF1R** | Colony Stimulating Factor 1 Receptor |
| **EAE** | experimental autoimmune encephalomyelitis |
| **IL34** | Interleukin 34 |
| **HSVTK** | Herpes Simplex Virus Thymidine Kinase |
| **MOG** | Major Oligodendrocyte Glycoprotein |
| **OCT** | optimal cutting temperature |
| **BSA** | Bovine Serum Albumin |
| **OPC** | oligodendrocyte progenitor cells |
| **TGFβ** | transforming growth factor-β |
| **GFAP** | Glial acidic fibrillary protein |
| **iNOS** | inducible Nitric Oxide Synthase |
| **EC** | Eriochrome cyanine |
| **Arg1** | Arginase 1 |
| **Th** | T helper |

## References

Ajami B, Bennett JL, Krieger C, McNagny KM, Rossi FM. 2011; Infiltrating monocytes trigger EAE progression, but do not contribute to the resident microglia pool. Nature neuroscience. 14:1142–1149. [PubMed: 21804537]

Bhasin M, Wu M, Tsirka SE. 2007; Modulation of microglial/macrophage activation by macrophage inhibitory factor (TKP) or tuftsin (TKPR) attenuates the disease course of experimental autoimmune encephalomyelitis. BMC Immunol. 8:10. [PubMed: 17634104]

Block ML, Zecca L, Hong JS. 2007; Microglia-mediated neurotoxicity: uncovering the molecular mechanisms. Nature reviews Neuroscience. 8:57–69. [PubMed: 17180163]

Bogie JF, Stinissen P, Hendriks JJ. 2014; Macrophage subsets and microglia in multiple sclerosis. Acta Neuropathol. 128:191–213. [PubMed: 24952885]

Borjini N, Fernandez M, Giardino L, Calza L. 2016; Cytokine and chemokine alterations in tissue, CSF, and plasma in early presymptomatic phase of experimental allergic encephalomyelitis (EAE), in a rat model of multiple sclerosis. J Neuroinflammation. 13:291. [PubMed: 27846891]

Bruttger J, Karram K, Wortge S, Regen T, Marini F, Hoppmann N, Klein M, Blank T, Yona S, Wolf Y, Mack M, Pinteaux E, Muller W, Zipp F, Binder H, Bopp T, Prinz M, Jung S, Waisman A. 2015; Genetic Cell Ablation Reveals Clusters of Local Self-Renewing Microglia in the Mammalian Central Nervous System. Immunity. 43:92–106. [PubMed: 26163371]

Byrne PV, Guilbert LJ, Stanley ER. 1981; Distribution of cells bearing receptors for a colony-stimulating factor (CSF-1) in murine tissue. J Cell Biol. 91:848–853. [PubMed: 6276411]

Chang A, Nishiyama A, Peterson J, Prineas J, Trapp BD. 2000; NG2-positive oligodendrocyte progenitor cells in adult human brain and multiple sclerosis lesions. J Neurosci. 20:6404–6412. [PubMed: 10964946]

Chang A, Tourtellotte WW, Rudick R, Trapp BD. 2002; Premyelinating oligodendrocytes in chronic lesions of multiple sclerosis. The New England journal of medicine. 346:165–173. [PubMed: 11796850]

Coniglio SJ, Eugenin E, Dobrenis K, Stanley ER, West BL, Symons MH, Segall JE. 2012; Microglial stimulation of glioblastoma invasion involves epidermal growth factor receptor (EGFR) and colony stimulating factor 1 receptor (CSF-1R) signaling. Molecular medicine. 18:519–527. [PubMed: 22294205]

Cunyat F, Rainho JN, West B, Swainson L, McCune JM, Stevenson M. 2016; Colony-Stimulating Factor 1 Receptor Antagonists Sensitize Human Immunodeficiency Virus Type 1-Infected Macrophages to TRAIL-Mediated Killing. Journal of virology. 90:6255–6262. [PubMed: 27122585]

Dagher NN, Najafi AR, Kayala KM, Elmore MR, White TE, Medeiros R, West BL, Green KN. 2015; Colony-stimulating factor 1 receptor inhibition prevents microglial plaque association and improves cognition in 3xTg-AD mice. J Neuroinflammation. 12:139. [PubMed: 26232154]

Dai X-M, Ryan GR, Hapel AJ, Dominguez MGm, Russell RG, Kapp S, Sylvestre V, Stanley ER. 2002; Targeted disruption of the mouse colony-stimulating factor 1 receptor gene results in osteopetrosis, mononuclear phagocyte deficiency, increased primitive progenitor cell frequencies, and reproductive defects. Blood. 99:111–120. [PubMed: 11756160]

Dheen ST, Kaur C, Ling EA. 2007; Microglial activation and its implications in the brain diseases. Current medicinal chemistry. 14:1189–1197. [PubMed: 17504139]

Di Bello IC, Dawson MR, Levine JM, Reynolds R. 1999; Generation of oligodendroglial progenitors in acute inflammatory demyelinating lesions of the rat brain stem is associated with demyelination rather than inflammation. Journal of neurocytology. 28:365–381. [PubMed: 10739577]

Elmore MR, Najafi AR, Koike MA, Dagher NN, Spangenberg EE, Rice RA, Kitazawa M, Matusow B, Nguyen H, West BL, Green KN. 2014; Colony-stimulating factor 1 receptor signaling is necessary for microglia viability, unmasking a microglia progenitor cell in the adult brain. Neuron. 82:380–397. [PubMed: 24742461]

Emerson MR, Gallagher RJ, Marquis JG, LeVine SM. 2009; Enhancing the ability of experimental autoimmune encephalomyelitis to serve as a more rigorous model of multiple sclerosis through refinement of the experimental design. Comparative medicine. 59:112–128. [PubMed: 19389303]

Erblich B, Zhu L, Etgen AM, Dobrenis K, Pollard JW. 2011; Absence of colony stimulation factor-1 receptor results in loss of microglia, disrupted brain development and olfactory deficits. PLoS One. 6:e26317. [PubMed: 22046273]

Feng X, Jopson TD, Paladini MS, Liu S, West BL, Gupta N, Rosi S. 2016; Colony-stimulating factor 1 receptor blockade prevents fractionated whole-brain irradiation-induced memory deficits. J Neuroinflammation. 13:215. [PubMed: 27576527]

Gensert JM, Goldman JE. 1997; Endogenous progenitors remyelinate demyelinated axons in the adult CNS. Neuron. 19:197–203. [PubMed: 9247275]

Heppner FL, Greter M, Marino D, Falsig J, Raivich G, Hovelmeyer N, Waisman A, Rulicke T, Prinz M, Priller J, Becher B, Aguzzi A. 2005; Experimental autoimmune encephalomyelitis repressed by microglial paralysis. Nature medicine. 11:146–152.

Hilla AM, Diekmann H, Fischer D. 2017; Microglia Are Irrelevant for Neuronal Degeneration and Axon Regeneration after Acute Injury. J Neurosci. 37:6113–6124. [PubMed: 28539419]

Hjelmstrom P, Juedes AE, Fjell J, Ruddle NH. 1998; B-cell-deficient mice develop experimental allergic encephalomyelitis with demyelination after myelin oligodendrocyte glycoprotein sensitization. J Immunol. 161:4480–4483. [PubMed: 9794370]

Huang JK, Jarjour AA, Nait Oumesmar B, Kerninon C, Williams A, Krezel W, Kagechika H, Bauer J, Zhao C, Baron-Van Evercooren A, Chambon P, Ffrench-Constant C, Franklin RJ. 2011; Retinoid X receptor gamma signaling accelerates CNS remyelination. Nature neuroscience. 14:45–53. [PubMed: 21131950]

Huang Y, Xu Z, Xiong S, Sun F, Qin G, Hu G, Wang J, Zhao L, Liang YX, Wu T, Lu Z, Humayun MS, So KF, Pan Y, Li N, Yuan TF, Rao Y, Peng B. 2018Repopulated microglia are solely derived from the proliferation of residual microglia after acute depletion. Nature neuroscience.

Kettenmann H, Hanisch UK, Noda M, Verkhratsky A. 2011; Physiology of microglia. Physiol Rev. 91:461–553. [PubMed: 21527731]

Kigerl K, Gensel J, Ankeny D, Alexander J, Donnelly D, Popovich P. 2009; Identification of two distinct macrophage subsets with divergent effects causing either neurotoxicity or regeneration in the injured mouse spinal cord. J Neurosci. 29:13435–13444. [PubMed: 19864556]

King IL, Dickendesher TL, Segal BM. 2009; Circulating Ly-6C+ myeloid precursors migrate to the CNS and play a pathogenic role during autoimmune demyelinating disease. Blood. 113:3190–3197. [PubMed: 19196868]

Klein D, Patzko A, Schreiber D, van Hauwermeiren A, Baier M, Groh J, West BL, Martini R. 2015; Targeting the colony stimulating factor 1 receptor alleviates two forms of Charcot-Marie-Tooth disease in mice. Brain. 138:3193–3205. [PubMed: 26297559]

Lee S, Shi XQ, Fan A, West B, Zhang J. 2018; Targeting macrophage and microglia activation with colony stimulating factor 1 receptor inhibitor is an effective strategy to treat injury-triggered neuropathic pain. Mol Pain. 14:1744806918764979. [PubMed: 29546785]

Levine JM. 1994; Increased expression of the NG2 chondroitin-sulfate proteoglycan after brain injury. J Neurosci. 14:4716–4730. [PubMed: 8046446]

Li J, Chen K, Zhu L, Pollard JW. 2006; Conditional deletion of the colony stimulating factor-1 receptor (c-fms proto-oncogene) in mice. Genesis. 44:328–335. [PubMed: 16823860]

Luo J, Elwood F, Britschgi M, Villeda S, Zhang H, Ding Z, Zhu L, Alabsi H, Getachew R, Narasimhan R, Wabl R, Fainberg N, James ML, Wong G, Relton J, Gambhir SS, Pollard JW, Wyss-Coray T. 2013; Colony-stimulating factor 1 receptor (CSF1R) signaling in injured neurons facilitates protection and survival. The Journal of experimental medicine. 210:157–172. [PubMed: 23296467]

Melief J, Schuurman KG, van de Garde MD, Smolders J, van Eijk M, Hamann J, Huitinga I. 2013; Microglia in normal appearing white matter of multiple sclerosis are alerted but immunosuppressed. Glia. 61:1848–1861. [PubMed: 24014207]

Mikita J, Dubourdieu-Cassagno N, Deloire MS, Vekris A, Biran M, Raffard G, Brochet B, Canron MH, Franconi JM, Boiziau C, Petry KG. 2011; Altered M1/M2 activation patterns of monocytes in severe relapsing experimental rat model of Multiple Sclerosis. Amelioration of clinical status by M2 activated monocyte administration. Mult Scler. 17:2–15. [PubMed: 20813772]

Mildner A, Mack M, Schmidt H, Bruck W, Djukic M, Zabel MD, Hille A, Priller J, Prinz M. 2009; CCR2+Ly-6Chi monocytes are crucial for the effector phase of autoimmunity in the central nervous system. Brain. 132:2487–2500. [PubMed: 19531531]

Miron VE, Boyd A, Zhao JW, Yuen TJ, Ruckh JM, Shadrach JL, van Wijngaarden P, Wagers AJ, Williams A, Franklin RJ, ffrench-Constant C. 2013; M2 microglia and macrophages drive oligodendrocyte differentiation during CNS remyelination. Nature neuroscience. 16:1211–1218. [PubMed: 23872599]

Mok S, Koya RC, Tsui C, Xu J, Robert L, Wu L, Graeber TG, West BL, Bollag G, Ribas A. 2014; Inhibition of CSF-1 receptor improves the antitumor efficacy of adoptive cell transfer immunotherapy. Cancer research. 74:153–161. [PubMed: 24247719]

Murase S, Hayashi Y. 1998; Expression pattern and neurotrophic role of the c-fms proto-oncogene M-CSF receptor in rodent Purkinje cells. J Neurosci. 18:10481–10492. [PubMed: 9852586]

Nimmerjahn A, Kirchhoff F, Helmchen F. 2005; Resting microglial cells are highly dynamic surveillants of brain parenchyma in vivo. Science. 308:1314–1318. [PubMed: 15831717]

Nishiyama A, Komitova M, Suzuki R, Zhu X. 2009; Polydendrocytes (NG2 cells): multifunctional cells with lineage plasticity. Nature reviews Neuroscience. 10:9–22. [PubMed: 19096367]

Nissen JC, Tsirka SE. 2016; Tuftsin-driven experimental autoimmune encephalomyelitis recovery requires neuropilin-1. Glia. 64:923–936. [PubMed: 26880314]

O'Loughlin E, Madore C, Lassmann H, Butovsky O. 2018Microglial Phenotypes and Functions in Multiple Sclerosis. Cold Spring Harb Perspect Med. :8.

Patel S, Player MR. 2009; Colony-stimulating factor-1 receptor inhibitors for the treatment of cancer and inflammatory disease. Current topics in medicinal chemistry. 9:599–610. [PubMed: 19689368]

Reynolds R, Dawson M, Papadopoulos D, Polito A, Di Bello IC, Pham-Dinh D, Levine J. 2002; The response of NG2-expressing oligodendrocyte progenitors to demyelination in MOG-EAE and MS. Journal of neurocytology. 31:523–536. [PubMed: 14501221]

Robinson AP, Harp CT, Noronha A, Miller SD. 2014; The experimental autoimmune encephalomyelitis (EAE) model of MS: utility for understanding disease pathophysiology and treatment. Handb Clin Neurol. 122:173–189. [PubMed: 24507518]

Salter MW, Stevens B. 2017; Microglia emerge as central players in brain disease. Nature medicine. 23:1018–1027.

Streit WJ, Walter SA, Pennell NA. 1999; Reactive microgliosis. Progress in neurobiology. 57:563–581. [PubMed: 10221782]

Swanborg RH. 1995; Experimental autoimmune encephalomyelitis in rodents as a model for human demyelinating disease. Clin Immunol Immunopathol. 77:4–13. [PubMed: 7554482]

Szalay G, Martinecz B, Lenart N, Kornyei Z, Orsolits B, Judak L, Csaszar E, Fekete R, West BL, Katona G, Rozsa B, Denes A. 2016; Microglia protect against brain injury and their selective elimination dysregulates neuronal network activity after stroke. Nat Commun. 7:11499. [PubMed: 27139776]

Torres L, Danver J, Ji K, Miyauchi JT, Chen D, Anderson ME, West BL, Robinson JK, Tsirka SE. 2016; Dynamic microglial modulation of spatial learning and social behavior. Brain, behavior, and immunity. 55:6–16.

Trapp BD, Peterson J, Ransahoff RM, Rudick R, Mork S, Bo L. 1998; Axonal Transection in the Lesions of Multiple Sclerosis. The New England journal of medicine. 338:278–285. [PubMed: 9445407]

Valdearcos M, Robblee MM, Benjamin DI, Nomura DK, Xu AW, Koliwad SK. 2014; Microglia dictate the impact of saturated fat consumption on hypothalamic inflammation and neuronal function. Cell reports. 9:2124–2138. [PubMed: 25497089]

Wu M, Nissen JC, Chen EI, Tsirka SE. 2012; Tuftsin promotes an anti-inflammatory switch and attenuates symptoms in experimental autoimmune encephalomyelitis. PLoS One. 7:e34933. [PubMed: 22529957]

Zawadzka M, Rivers LE, Fancy SP, Zhao C, Tripathi R, Jamen F, Young K, Goncharevich A, Pohl H, Rizzi M, Rowitch DH, Kessaris N, Suter U, Richardson WD, Franklin RJ. 2010; CNS-resident glial progenitor/stem cells produce Schwann cells as well as oligodendrocytes during repair of CNS demyelination. Cell stem cell. 6:578–590. [PubMed: 20569695]

Zhang Z, Zhang ZY, Schittenhelm J, Wu Y, Meyermann R, Schluesener HJ. 2011; Parenchymal accumulation of CD163+ macrophages/microglia in multiple sclerosis brains. Journal of neuroimmunology. 237:73–79. [PubMed: 21737148]

Zrzavy T, Hametner S, Wimmer I, Butovsky O, Weiner HL, Lassmann H. 2017; Loss of 'homeostatic' microglia and patterns of their activation in active multiple sclerosis. Brain. 140:1900–1913. [PubMed: 28541408]

## HIGHLIGHTS

- Microglial depletion attenuates the physical and pathological hallmarks of EAE

- Microglia-depleted animals retain more mature, myelinating oligodendrocytes

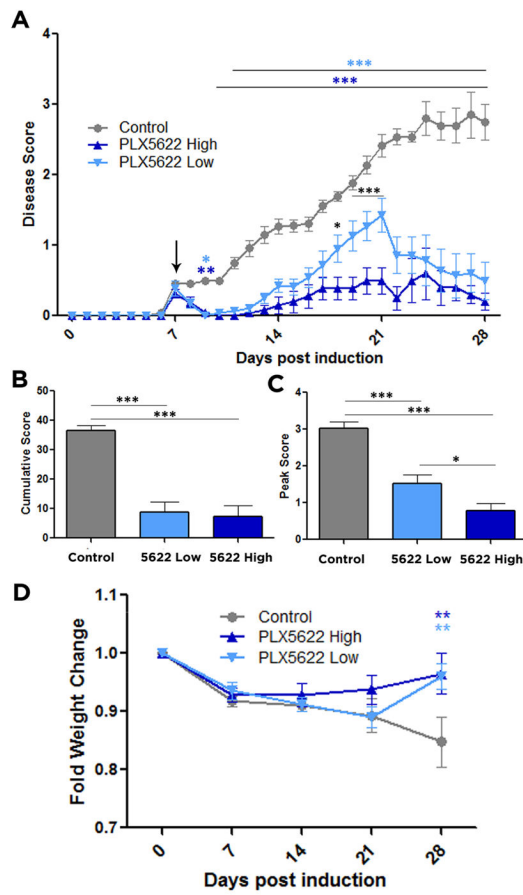- Continuous treatment maintains depletion and disease modifying effects

**Figure 1. Microglial depletion reduces EAE disease score and weight loss**

EAE was induced by injection of $MOG_{35-55}$ in CFA and pertussis toxin. Animals were fed control food or food containing a high or low dose of PLX5622 on day 7 after MOG immunization. Comparisons are between control and high-dose treated mice (dark blue asterisks), control and low-dose treated mice (light blue asterisks), and high- and low-dose treated mice (black asterisks) **(A)**. Cumulative scores over the 28 days **(B)** and peak scores **(C)** were compared between all groups. **(D)** Weight changes were recorded and compared between control and PLX5622 high- and low-dose treated mice. All weights were plotted as percentages of day 0 weights. Data are mean ± SEM, and analyzed by one-way ANOVA followed by a Bonferroni post-test **(A, D)** or two-tailed T test **(B, C)**. n= 12–16, *, $p<0.05$; **, $p<0.01$, ***, $p<0.001$.
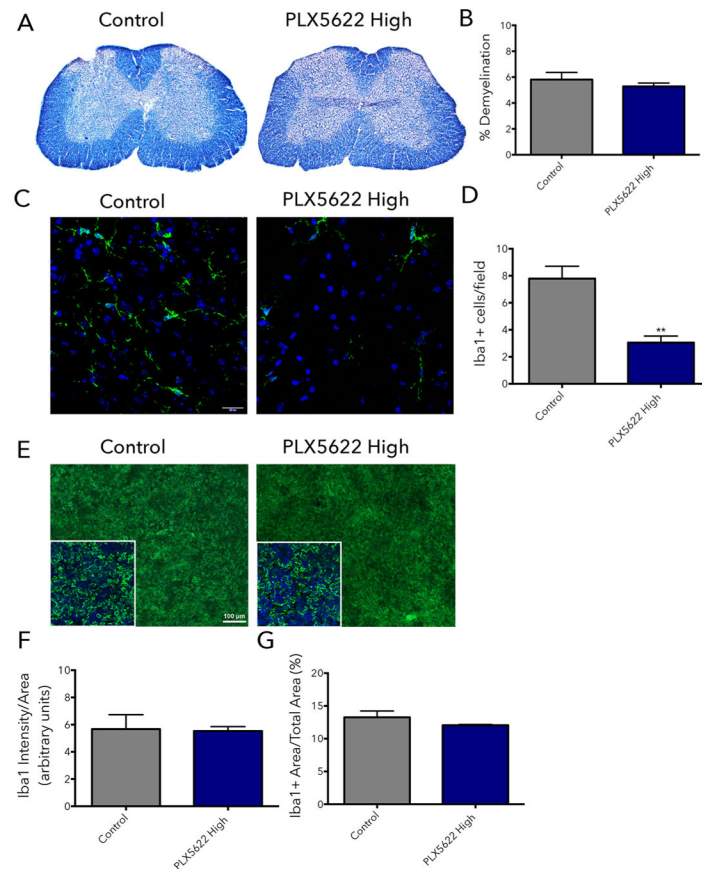
**Figure 2. Partial microglial depletion rapidly alleviates EAE symptoms**
EAE was induced by injection of MOG$_{35-55}$ in CFA (day 0 and 7) and pertussis toxin (day 0 and 2). Animals were placed on control food or food containing 1200 mg/kg of PLX5622 starting on day 7 after EAE induction. On day 9, mice were euthanized and the spinal cord and spleen were collected for histological analysis. To visualize demyelination, 20 μm frozen spinal cord sections were stained with eriochrome cyanine **(A)**. Demyelinated area was quantified using thresholding in ImageJ **(B)**. To evaluate microglia and macrophage depletion in the spinal cord **(C)** and macrophage depletion in the spleen **(E)**, 20 μm frozen tissue sections were stained using Iba1 antibody (green). For the spinal cord, total numbers of Iba1+ cells per field were counted **(D)**. For the spleen, the mean fluorescence intensity of Iba1+ cells **(F)** and the percent area positive for Iba1 staining **(G)** were calculated in ImageJ. All data are mean ± SEM, n = 4. **p<0.01.
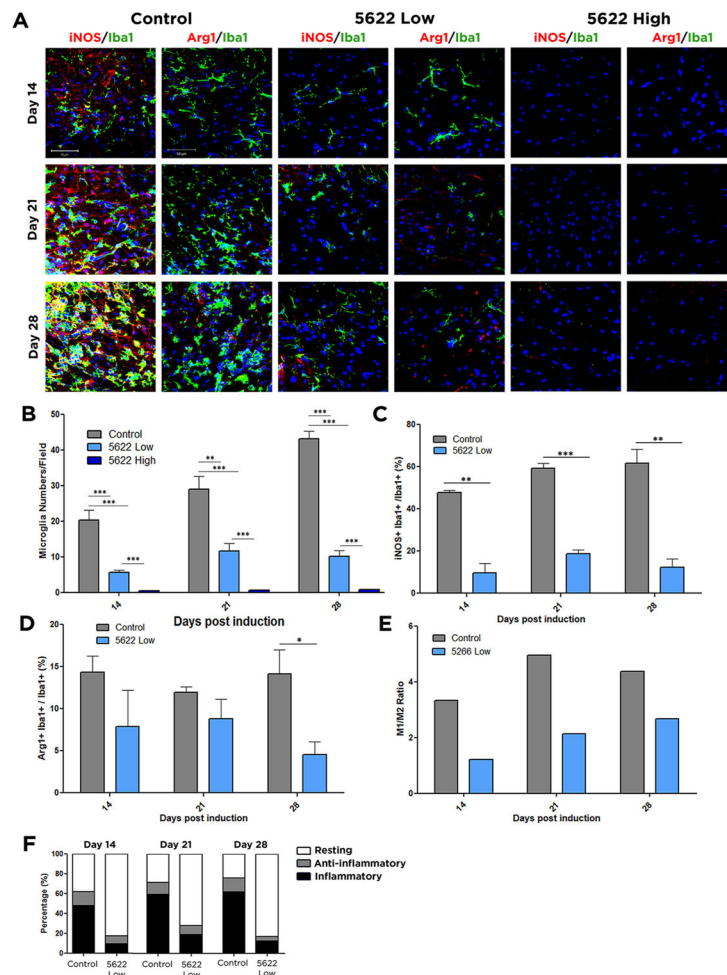
**Figure 3. Microglial populations are less inflammatory following CSF1R inhibition**
Frozen spinal cord sections were isolated from control, PLX5622 high dose, or PLX5622 low dose treated mice at day 14, 21, and 28 days post induction of EAE. Microglia were stained using the marker Iba1 (green). To observe inflammatory cells, tissue was costained for iNOS (red), and for anti-inflammatory cells costained for Arg1 (red). DAPI is shown in blue **(A)**. Total numbers of microglia per field are shown in **(B)**. Inflammatory cells, identified by double staining for iNOS and Iba1, were quantified in **(C)**, and anti-inflammatory cells, identified by double staining for Arg1 and Iba1 were quantified in **(D)**. The ratio of the percentages of inflammatory cells relative to anti-inflammatory cells is shown in **(E)**, and percentages of each population after treatment are indicated in **(F)**. Data are mean ± SEM, and analyzed by one-way ANOVA followed by a Bonferroni post-test. n=3, *, $p<0.05$; **, $p<0.01$; ***, $p<0.001$; Scale bar: 50 μm.
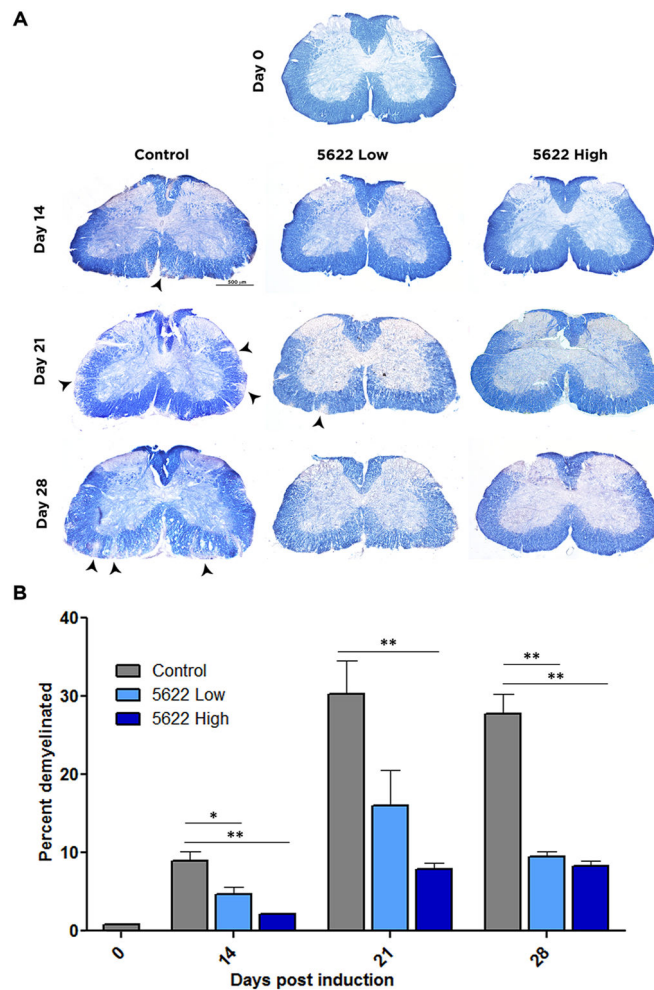
**Figure 4. Microglial depletion reduces spinal demyelination in EAE**
Frozen spinal cord sections were isolated from control, PLX5622 high dose, or PLX5622 low dose treated mice at day 14, 21, and 28 days post induction of EAE. To visualize demyelination, eriochrome cyanine was used. Myelinated regions of the white matter stain blue, where demyelinated regions are indicated by diminished color. Images of full coronal sections are shown, with demyelinated areas denoted by arrowheads **(A)**. Demyelinated areas were measured using ImageJ and quantified in **(B)**. Data are mean ± SEM, and analyzed by one-way ANOVA followed by a Bonferroni post-test. n=3, *, $p<0.05$; **, $p<0.01$, Scale bar: 500 μm.
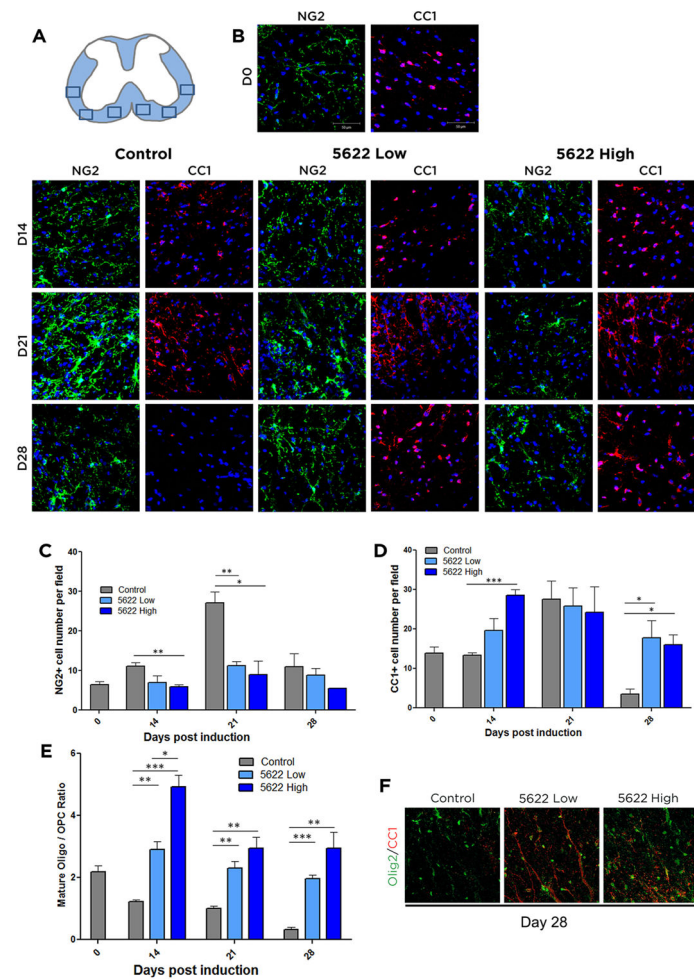
**Figure 5. Oligodendrocyte populations are shifted towards a mature phenotype following CSF1R inhibition**

Frozen spinal cord sections were isolated from control, PLX5622 high dose, or PLX5622 low dose treated mice at day 14, 21, and 28 days post induction of EAE. Regions where images were taken is depicted in (**A**). To visualize OPCs, tissue was stained for NG2 (green). To visualize mature oligos, tissue was stained with CC1 (red. Cell nuclei are shown in blue (DAPI) (**B**). Numbers of NG2+ (**C**), CC1+ (**D**), and the ratio of CC1+/NG2+ cells per field (**E**) were calculated. Tissue isolated on D28 post-EAE induction was stained for Olig2 (green) to denote all oligodendrocyte lineage cells, and CC1 (red) to denote mature oligodendrocytes (**F**). Data are mean ± SEM, and analyzed by one-way ANOVA followed by a Bonferroni post-test. n=3, *, $p<0.05$; **, $p<0.01$, ***, $p<0.001$. Scale bar: 50 μm.
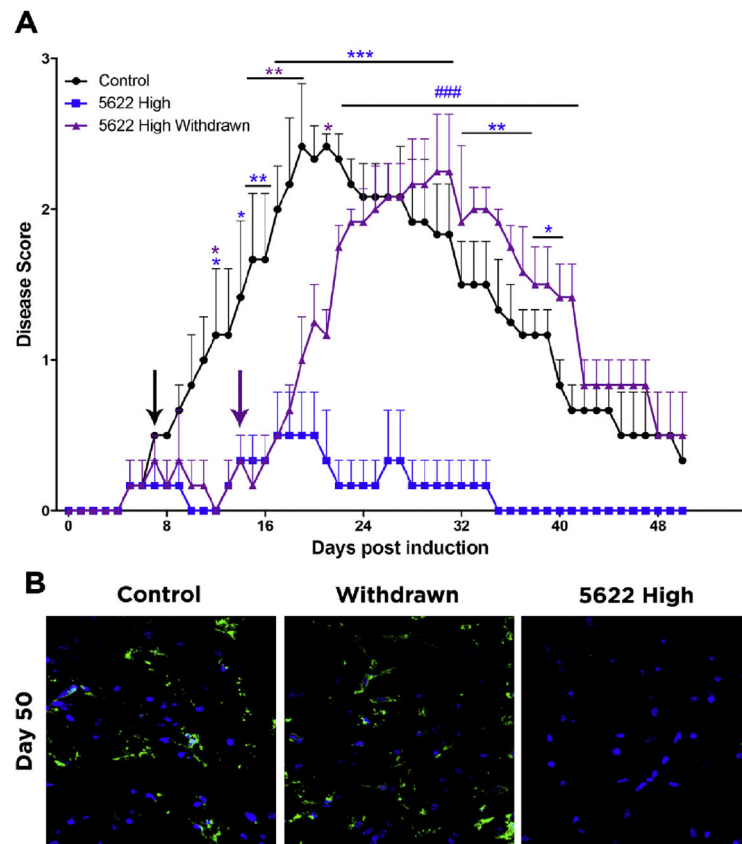
**Figure 6. Withdrawal of PLX5622 causes the emergence of EAE symptoms**
(**A**) EAE was induced by injection of $MOG_{35-55}$ in CFA and pertussis toxin. Animals were fed control food or food containing a high dose of PLX5622 on day 7 (black arrow) after MOG immunization. On day 14 (purple arrow) after EAE induction, PLX Withdrawn animals were switched from high dose PLX5622 to control food. Comparisons are between control and mice maintained on PLX5622 high dose (blue asterisks), control and PLX Withdrawn mice (purple asterisks), and PLX5622 high-dose and withdrawn mice (blue pound signs) Data are mean ± SEM. n=3. *$p<0.05$, **$p<0.01$, ***$p<0.001$, ###$p<0.001$. (**B**) At day 50, microglia and macrophages were visualized in the lumbar spinal cord by Iba1 immunofluorescence.
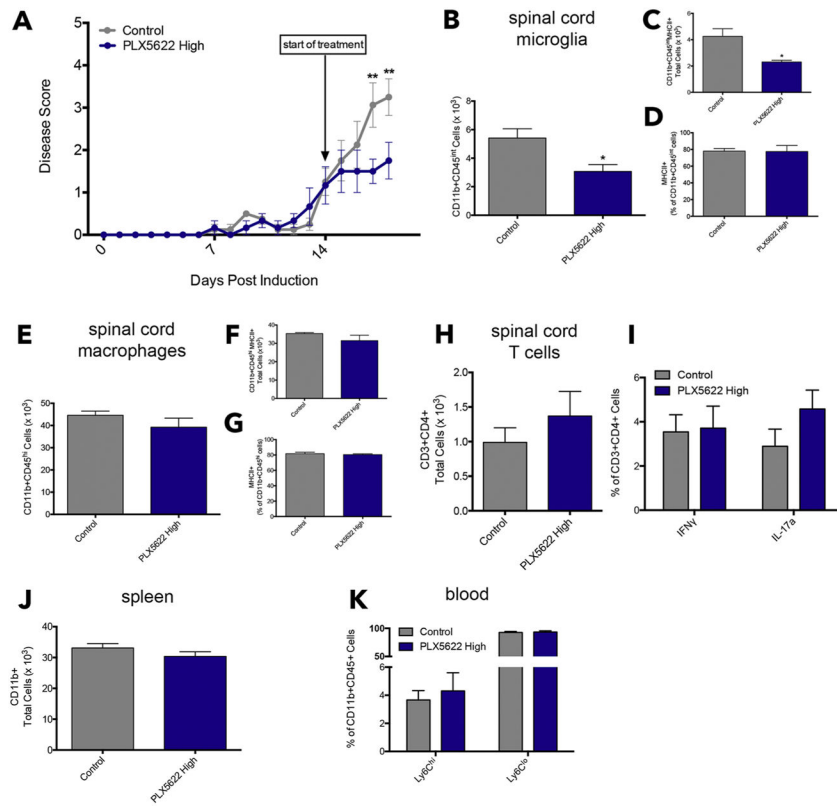
**Figure 7. Therapeutic treatment with the CSF1R inhibitor attenuates EAE and rapidly depletes microglia, but not macrophages**

EAE was induced by injection of $MOG_{35-55}$ in CFA and pertussis toxin. Animals were placed on control chow or chow containing 1,200 mg/kg PLX5622 starting on Day 14 after the emergence of EAE symptoms to model a therapeutic treatment regimen (**A**). On Day 18, mice were euthanized and spinal cord, spleen, and blood were collected for flow cytometric analysis. The spinal cord was analyzed for the presence of microglia, macrophages, and T cells. Microglia were marked by CD11b+CD45$^{int}$ expression (**B**) and total MHCII+ populations of microglia were quantified and expressed as a percentage of total microglia (**C & D**). Macrophages were marked by CD11b+CD45$^{hi}$ expression (**E**) and MHCII+ antigen-presenting cells were evaluated by total numbers and percentage (**F & G**). T helper cells were evaluated by CD3 and CD4 expression (**H**) and intracellular expression of IFNγ and IL-17a were used to distinguish Th1 and Th17 subsets (**I**). Spleens were analyzed for total CD11b+ cells (**J**). Ly6C$^{hi}$ and Ly6C$^{lo}$ expression was analyzed within the CD11b+CD45+ population in whole blood (**K**). All data are mean ± SEM, n = 3–4. *p<0.05, **p<0.01.